Study the Effects of Micro-Textured Cutting Tool on Surface Quality and Tool Wear when Machining Aluminium Alloy 7075-T6

Seyed Hasan Musavi
Amirkabir University of Technology
Majid Sepehrikia
Iran University of Science and Technology
Seyed Ali Niknam (seyed-ali.niknam@polymtl.ca)
Polytechnique Montreal
Behnam Davoodi
Iran University of Science and Technology

Research Article

Keywords: 7075 aluminum alloy, micro-texture, tool wear, dry machining, minimum quantity lubrication

Posted Date: June 28th, 2021

DOI: https://doi.org/10.21203/rs.3.rs-617721/v1

Study the effects of micro-textured cutting tool on surface quality and tool wear when machining aluminium alloy 7075-T6

Seyed Hasan Musavi[1], Majid Sepehrikia[2], Seyed Ali Niknam[2,3*], Behnam Davoodi[2]

1. Department of Mechanical Engineering, Amirkabir University of Technology, Tehran, Iran.
2. Sustainable manufacturing systems research laboratory, Department of Mechanical Engineering, Iran University of Science and Technology.
3. Department of Mechanical Engineering, Polytechnique Montreal, Canada.

*Corresponding author: saniknam@iust.ac.ir; seyed-ali.niknam@polymyl.ca

Abstract

Due to the wide applications of aluminum alloy in numerous industrial sectors and products, significant attention has been paid by many researchers to improve the production and manufacturing aspects of aluminium alloys and related products. One of the main concerns in this regard is the cutting tool life when machining aluminium alloys. This work aims to present the capability and performance of a new strategy of life improvement in the tungsten carbide inserts by creating micro-textured grooves on their surface. For this purpose, the laser was used to create the different morphologies of textures on the insert surfaces. The grooves were created with different distances in parallel to the cutting edge on the tool rake face. The effects of fabricated grooves on the tool wear attributes were discussed in three directions, including the main edge (x-direction), side edge (y-direction), and radial (in the direction of 45 degrees) and the effect of these grooves/textures on the surface roughness attributes were also studied. To that end, experimental works were performed under dry and minimum quantity lubrication (MQL), as well as three levels of cutting speed, feed rate, and grooves distance. The experimental results were compared with those measured under non-textured inserts. Finally, the obtained results were statistically analyzed, and the empirical models were formulated. Experimental results indicated that micro-textured inserts in both MQL and dry conditions led to surface quality and tool wear as compared to readings made under non-textured inserts.

Keywords:
7075 aluminum alloy, micro-texture, tool wear, dry machining, minimum quantity lubrication

1. Introduction

Due to the special properties of aluminum alloy, such as low weight, good stiffness, low production cost, and good corrosion resistance, this alloy is widely used in numerous industrial sectors. However, specific mechanical properties of these alloys, in principle low melting temperatures and low strength, may tend to increase the tool wear size in machining processes, and effectively machining difficulties may occur [1, 2]. For this reason, the main aims of the recent research studies on aluminium alloys were devoted to finding solutions to increase production efficiency and reducing machining costs.

Several wear mechanisms appear in the cutting tools used in machining aluminum. The main type is adhesion [3]. This wear mechanism is so common that it occurs at the first contact between the tool and workpiece [4]. Intense adhesion wear increases due to the atom transition between tool and chip interfaces, resulting in a chemical bonding. At higher levels of pressure, the interaction layers reinforce, which leads to an extension of the adhesion zone [5]. To improve the wear conditions, cutting fluids are used in large volumes to reduce the temperature in the machining zone, lubricate the tool-workpiece interface, and clean the cutting zone from chips [6]. Although cutting fluids present significant benefits, it can not always be considered the first solution for tool wear reduction. Using cutting fluid in the machining of soft materials (e.g., aluminum alloys) may change the angle of cutting edges by creating a built-up edge [7, 8].

Applying texture on the tool rake face in micron size can be a novel method for improving the tool wear condition in machining soft alloy [9, 10]. Reduction in tool-workpiece contact length seems to be the main reason for the decrease in adhesion wear when using the micro-textured insert [11]. The micro-textured inserts have significant effects on cooling and lubrication performance in the cutting zone, which may decrease the adhesion wear and cutting force up to 30% [12, 13]. Experimental studies showed that regular textures on the tool surface reduce the tool-chip interaction's actual surface, consequently decreasing the friction coefficient up to 42%, and the generated heat up to 37%. By temperature subsiding, the condition of chip welding on the tool surface can be decreased; thereby, the anti-wear property of cutting tools might be improved [14, 15]. This behavior can be attributed to the storage of cutting fluid in the textures and produce a high hydrodynamic pressure during sliding between tool rake face and removed chip [16].

Zhang et al. [1] studied the influence of texture on the adhesion wear properties of tungsten carbide cutting tool with TiAlN coating in turning operation. The results showed that both micro and micro-nano textures provide better anti-wear properties than non-textured cutting tools. Arulkirubakaran et al. [12] examined the impact of micro-textured cutting tools on machining performance. Under the use of textured tools, cutting temperature, tool-chip contact length, and cutting force were lower than readings under the non-textured cutting tool. In addition, less tool wear and lower friction coefficient were observed in all

types of micro-textured cutting tools. Kummel et al. [18] fabricated the micro-textures on the tool rake face and evaluated the influences of the developed tools on the BUE stabilization and tool wear mechanisms. Their evaluation showed that the wear behavior was improved compared to non-textured tools by creating dimple texture and groove textures. Fang et al. [19] evaluated the impact of the micro-texture on the cooling-lubrication performance when a high-pressure jet of cutting fluid was used. The experimental results revealed that the micro-texture could control the cutting temperature using the higher ability of the cutting fluid transfer. Consequently, the use of micro-textured cutting tools generally may tend to decreased flank as well as crater wear in comparison with readings made from non-textured cutting tools.

According to the literature review, there is no experimental and statistical work on estimating wear length at the different directions of the micro-textured cutting tool in machining aluminium alloys. Therefore, in the present work, the tool wear length in three directions and surface roughness of the workpiece were compared with the non-textured tools in the machining of AA7075. For a more detailed study, two methods of dry and MQL, as well as three levels of cutting speed, feed rate, and groove distance, have been used. Finally, the obtained experimental results were statistically analyzed using statistical software to extract their statistical equations, and analysis of variance was used to evaluate the accuracy of these equations.

2. Materials and Equipment

Solid rods of 7075 aluminum alloy was used as the workpiece materials. The mechanical properties and chemical composition of the AA7075 (Table 1) were extracted from energy-dispersive X-ray spectroscopy analysis and mechanical tests conducted at the Iran University of Science and Technology in collaboration with local automotive and energy industries.

Table 1 Specifications of the AA7075

Workpiece materials (wt%)	Zn %6, Mg %3, Cu %2, Fe %0.6, Si %0.5, Mn %0.4, Cr %0.3, Ti %0.3, Al base
Mechanical property	Thermal conductivity (W/m ° C) 130 Tensile strength (MPa) 572 Young’ s modulus (GPa) 72 Yield strength (MPa) 503 Melting point (° C) 600 Density (kg/m3) 2800 Hardness (HV) 173
Workpiece geometry	Circular cross-section Diameter (mm) 40 Length (mm) 330 Machining length (mm) 70

The cemented uncoated carbide insert SNMA 120408/ grade code of GC3205, manufactured by Sandvik company based on ISO3685:1993 standard, was used. The rake angle of zero degrees was used. After mounting on the PCNL 2525 M12 tool holder, the inserts' clearance angle and rake angle were changed to - 6° and 6°, respectively. The surface roughness was measured by a TR-200 plus tester. Three points perpendicular to the cutting depth orientation were considered to conduct precise measurement, and the average values were reported. The maximum and minimum values will also be reported in diagrams representing the larger and smaller amounts of surface roughness measured.

A pressurized injection mode was performed to achieve a better penetration of cutting fluid to the tool-workpiece interface. For this aim, the minimum quantity lubrication (MQL) method was introduced in the present work. The MQL machine was designed and developed by the authors. In this machine, the cutting fluid combines with the compressed air in two steps to produce a perfect spray. The flow rate and pressure can be set at 100-800 cm^3/h and 200-700 kPa, respectively. The accuracy of the designed MQL machine was verified through initial experimental tests. Fig. 1 shows the setup of the turning process and the position of the MQL nozzle to the texture direction.

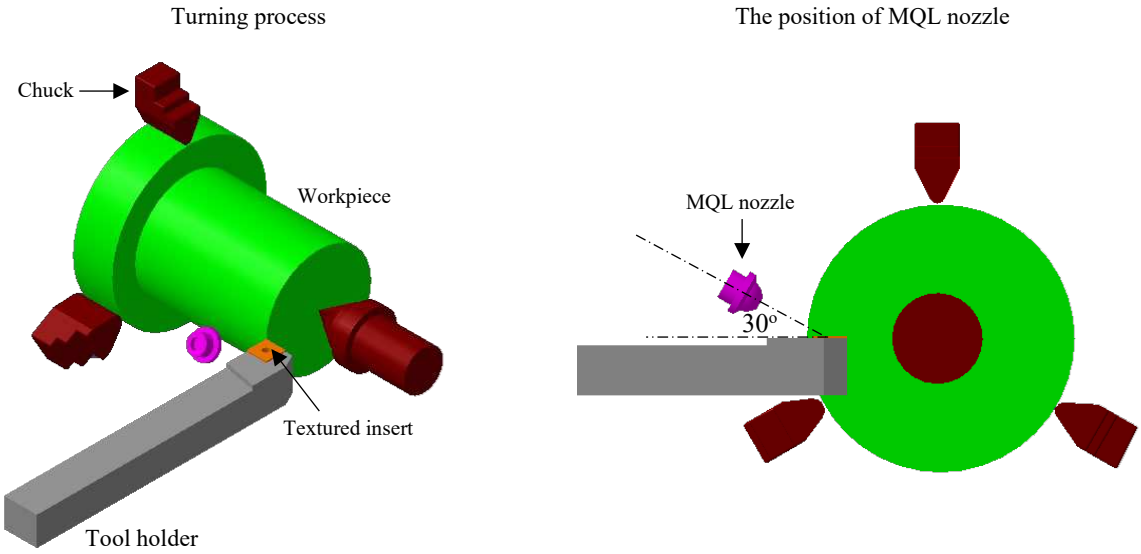

Fig. 1 Schematic overview of the turning process

3. Tool texture fabrication

Laser beam machining was used to create the texture on the tool rake face, as shown in Fig. 2. The utilized laser was an FBL20 engraving machine. The specifications of this machine include voltage, frequency, and electric current of 220V, 50kHz, and 4A, respectively. The maximum power consumption and the produced wavelength of the beam are 20W and 1065nm, respectively. Before performing the laser

machining process on the tool rake face, the insert must be clean and free of additional impurities. For this purpose, the following two steps were conducted before and after the texture creation:

- To clean the tool's surface from any grease, the inserts were placed in an ultrasonic bath of ethanol for half an hour. Under such conditions, any grease and impurities could be removed, and the inserts could undergo laser machining.
- Due to the melting mechanism of chip removal in the laser machining, the materials of the tool that have been melted remain insignificantly between the grooves. The inserts were then placed in an ultrasonic bath with acetone, and it was vibrated for an hour.

Fig. 3 shows the schematic and real image of the tool rake face before and after laser surface texturing.

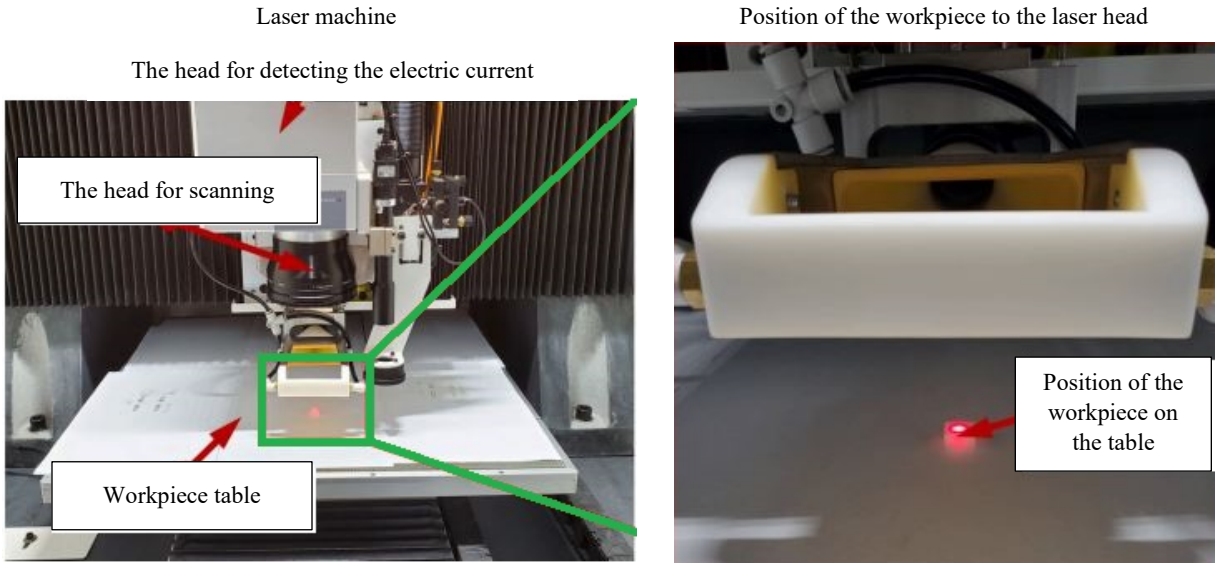

Fig. 2 Laser beam machining tool

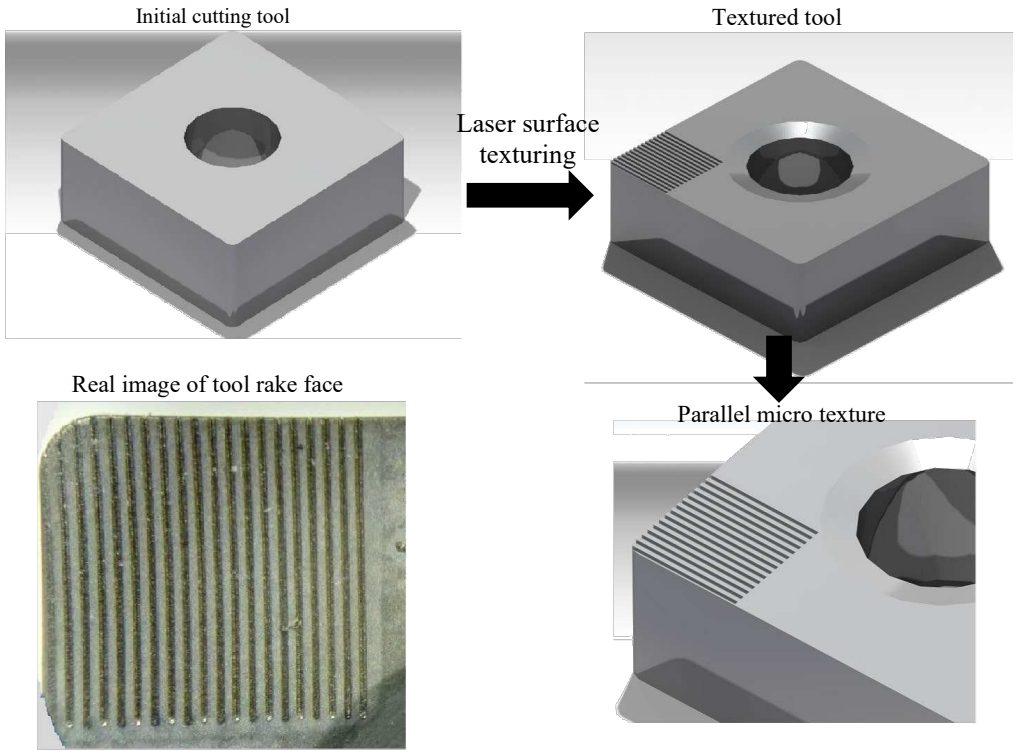

Fig. 3 The overviews simulation and fabricated textured inserts

4. Design of experiments

To investigate the effect of cutting parameters and lubrication conditions on tool wear and surface roughness in machining of 7075 aluminum alloy, three factors, including cutting speed (Vc), feed rate (f), and grooves distance (d) were considered in three levels under dry and MQL conditions. Due to many experiments, the response surface methodology (RSM) was used to design the experimental model. The response surface methodology is one of the optimization methods that use a set of mathematical and statistical techniques to model problems, and it does not only reduce the number and related expenses of experimental tests, but it also predicts the natural approach of the optimization process, which is often nonlinear [20]. A standard response surface methodology called Box-Wilson Central Composite Design (CCD) was used in this study. Machining parameters and their levels are shown in Table 2. The specifications of the designed RSM are presented in Table 3.

Table 2 Cutting parameters and their levels

Cutting parameters	Levels		
	Level 1	Level 2	Level 3
Cutting speed v_c (m/min)	100	125	150
Feed rate *f* (mm/rev)	0.1	0.15	0.2
Groves distance d (μm)	100	200	300

Table 3 RSM specifications

Total runs	Blocks	Factors	Cube points	Center points in a cube	Axial points	Center points in axial	Alpha
20	2	3	8	4	6	2	1.633

5. Results and discussion

Tables 4 and 5 show the cutting parameters and all the measured tool wear values in the three directions (as shown in Fig. 4) and surface roughness, respectively. Tables 4 and 5 belong to MQL mode, but full details about other conditions were reported in the appendix. The obtained results were statistically analyzed using Design Expert statistical software, and mathematical models were then formulated.

Table 4 Matrix L20 of response surface methodology of wear results in MQL method using a textured tool

Test number	Matrix L20			Blocks	F_1 V_c (m/min)	F_2 f (mm/rev)	F_3 d (µm)	Tool wear		
	F_1	F_2	F_3					TW-x (mm)	TW-y (mm)	TW-r (mm)
1	0.000	0.000	1.633	2	125	0.15	300	0.74	0.70	0.48
2	0.000	0.000	0.000	1	125	0.15	200	0.49	0.477	0.31
3	0.000	0.000	0.000	2	125	0.15	200	0.5	0.48	0.31
4	0.000	0.000	-1.633	2	125	0.15	100	0.43	0.40	0.27
5	-1.633	0.000	0.000	2	100	0.15	200	0.60	0.57	0.40
6	1.000	1.000	-1.000	1	150	0.20	100	0.45	0.43	0.28
7	-1.000	1.000	-1.000	1	100	0.20	100	0.65	0.62	0.43
8	1.000	-1.000	-1.000	1	150	0.10	100	0.40	0.35	0.25
9	0.000	0.000	0.000	1	125	0.15	200	0.49	0.45	0.31
10	1.633	0.000	0.000	2	150	0.15	200	0.57	0.55	0.36
11	0.000	1.633	0.000	2	125	0.20	200	0.62	0.60	0.47
12	0.000	0.000	0.000	1	125	0.15	200	0.51	0.49	0.33
13	1.000	-1.000	1.000	1	150	0.10	300	0.60	0.55	0.40
14	0.000	0.000	0.000	2	125	0.15	200	0.5	0.48	0.31
15	1.000	1.000	1.000	1	150	0.20	300	0.65	0.60	0.45
16	-1.000	-1.000	1.000	1	100	0.10	300	0.73	0.70	0.48
17	0.000	-1.633	0.000	2	125	0.10	200	0.43	0.40	0.27
18	0.000	0.000	0.000	1	125	0.15	200	0.5	0.47	0.32
19	-1.000	1.000	1.000	1	100	0.20	300	0.76	0.73	0.5
20	-1.000	-1.000	-1.000	1	100	0.10	100	0.55	0.52	0.35

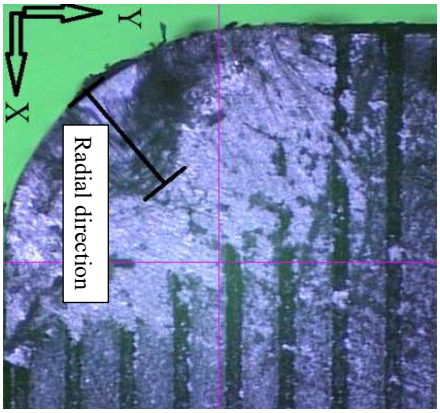

Fig. 4 The wear directions on the tool rake face

5.1. Development and analyses of mathematical models

In the response surface methodology, the relationship between the response and the independent variables are unknown. Therefore, the first step in the RSM is to find the appropriate approximation for the correct relationship between the response and the set of independent variables. Low-order polynomials are usually used in an area of independent variable values [20, 21]. In RSM, the relationship between input parameters (V_c, f, and d) and output response (Y) can be expressed with Equation (1):

$$Y = F(a_f; d; V_c) \quad (1)$$

Table 5 Matrix L20 of response surface methodology of roughness results in MQL method using textured tool

Test number	Matrix L20			Blocks	F_1 V_c (m/min)	F_2 f (mm/rev)	F_3 d (μm)	Roughness	
	F_1	F_2	F_3					R_a (μm)	Rz (μm)
1	0.000	0.000	1.633	2	125	0.15	300	0.689	5.013
2	0.000	0.000	0.000	1	125	0.15	200	0.411	2.635
3	0.000	0.000	0.000	2	125	0.15	200	0.419	2.641
4	0.000	0.000	-1.633	2	125	0.15	100	0.375	2.342
5	-1.633	0.000	0.000	2	100	0.15	200	0.512	3.817
6	1.000	1.000	-1.000	1	150	0.20	100	0.394	2.421
7	-1.000	1.000	-1.000	1	100	0.20	100	0.571	4.542
8	1.000	-1.000	-1.000	1	150	0.10	100	0.311	2.181
9	0.000	0.000	0.000	1	125	0.15	200	0.408	2.642
10	1.633	0.000	0.000	2	150	0.15	200	0.462	3.083
11	0.000	1.633	0.000	2	125	0.20	200	0.507	3.579
12	0.000	0.000	0.000	1	125	0.15	200	0.412	2.637
13	1.000	-1.000	1.000	1	150	0.10	300	0.495	3.275
14	0.000	0.000	0.000	2	125	0.15	200	0.416	2.649
15	1.000	1.000	1.000	1	150	0.20	300	0.546	4.124
16	-1.000	-1.000	1.000	1	100	0.10	300	0.673	4.867
17	0.000	-1.633	0.000	2	125	0.10	200	0.382	2.407
18	0.000	0.000	0.000	1	125	0.15	200	0.412	2.647
19	-1.000	1.000	1.000	1	100	0.20	300	0.794	5.293
20	-1.000	-1.000	-1.000	1	100	0.10	100	0.427	2.821

In the present study, to predict the approximate response values, a second-order polynomial regression model was used, and the regression model for the number of K factors was presented as Equation (2):

$$Y = B_0 + \sum_{i=1}^{k} B_i x_i + \sum_{i,j=1}^{k} B_{ij} x_i x_j + \sum_{i=1}^{k} B_{ii} {x_i}^2 \quad (2)$$

B_0 is the free term, B_i is a linear coefficient, B_{ii} is a quadratic term, B_{ij} is the interaction factor, and x_i indicates input parameters [22, 23]. The values of nonlinear coefficients were calculated by the regression method according to the experimental data in Table 4. By replacing the values in Equation (2), the final tool wear models in the X direction for MQL machining with the textured tool for coded and actual parameters are presented as Equations (3) and (4), respectively:

$$Y = 0.51 - 0.062V_c + 0.042f + 0.1d - 0.0037V_cf + 0.014V_cd - 0.0087fd + 0.050{V_c}^2 - 0.0095f^2 + 0.050d^2 \quad (3)$$

$$TWx = 1.9028 - 0.023V_c + 2.7104f - 0.0014d - 0.003V_cf + 0.000005V_cd - 0.0017fd + 0.0000807{V_c}^2 - 3.1818f^2$$

$$+0.00000504d^2 \quad (4)$$

Also, the final tool wear models in Y and radial directions are Equations (5) and (6), respectively.

$$TWy = 1.833 - 0.02344V_c + 2.62f - 0.00076d + 0.000V_cf + 0.000004V_cd - 0.0025fd + 0.00008{V_c}^2 - 4.000f^2 + 0.000004d^2 \quad (5)$$

$$TWr = 1.30605 - 0.013671V_c - 0.91727f - 0.000779d - 0.002V_cf + 0.000006V_cd - 0.001fd + 0.000044{V_c}^2 + 7.0909f^2 + 0.0000022d^2 \quad (6)$$

Fig. 5a shows the normal probability for tool wear results in X direction using the MQL method with the textured tool. The uniform distribution of tool wear results relative to the straight line indicates the standard scatter of the data and the accuracy of the predicted Equation for the wear of micro-textured tool in MQL machining. Fig. 5b represents the distribution diagram of the wear results in the X direction for the two real and predicted states by Design-Expert software in the MQL machining process with the textured tool.

The horizontal axis of the diagram represents the actual results (experimental tests), and the vertical axis represents the results predicted by the statistical software. The centerline drawn in the diagram indicates that the predicted results are very close to the actual ones if the results are close to it. According to Fig. 5, it can be easily concluded that RSM has a very high accuracy compared to the laboratory results.

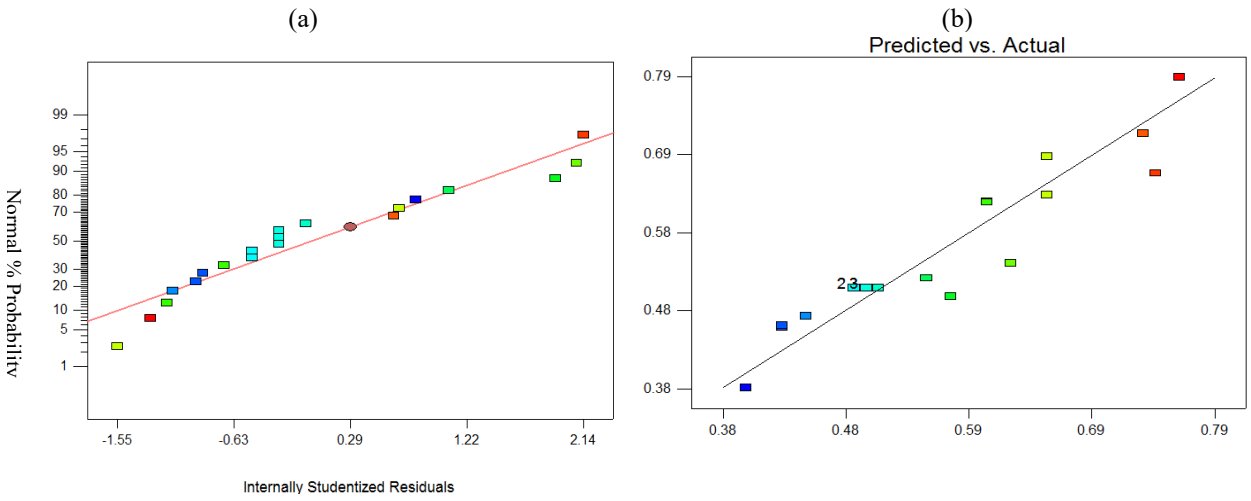

Fig. 5 Normal probability for tool wear results in X direction using MQL method with the textured tool

The analysis of variance (ANOVA) for tool wear in different directions for MQL machining with the textured tool is presented in Table 6 to Table 8. F-values and Probability>F in the analysis of variance are investigated to check the quality of the models. The F-value of the present analysis is 8.50. According to Table 6 and given the critical F-value of 4.66 for the data, the computed F-values demonstrate that the quadratic regression model is appropriate for predicting tool wear. In addition, the Probability>F value for the model is 0.0012, which indicates that the fitted model is meaningful. The values of percentage contribution are also presented in Table 6. The groove distance is the most effective parameter on tool wear in MQL machining with the micro-textured tool. The numerical value of grooves distance on tool wear in the X direction is more than 57%. Cutting speed and feed rate have 22.2% and 10.2% contribution to tool wear variation, respectively.

Table 6 ANOVA table of tool wear in X direction for MQL machining with textured tool

Source	Sum of squares	DF	Mean square	F-value	Prob>F	Degree of significance	Contribution (%)
Model	0.19	9	0.022	8.50	0.0012	Significant	
V_c	0.038	1	0.038	15.18	0.0030		22.2
f	0.018	1	0.018	6.96	0.0248		10.2
d	0.100	1	0.100	39.48	<0.0001		57.9
$V_c \times f$	1.125E-4	1	1.125E-4	0.044	0.8373		0.06
$V_c \times d$	1.513E-3	1	1.513E-3	0.60	0.4576		0.90
$f \times d$	6.125E-4	1	6.125E-4	0.24	0.6335		0.35
V_c^2	7.001E-3	1	7.001E-3	2.76	0.1274		4.00
f^2	2.506E-4	1	2.506E-4	0.099	0.7596		0.14
d^2	7.001E-3	1	7.001E-3	2.76	0.1274		4.00
Residual Error	0.025	10	2.533E-3				0.25
Total	0.22	19					100

Table 7 ANOVA table of tool wear in Y direction for MQL machining with textured tool

Source	Sum of squares	DF	Mean square	F-value	Prob>F	Degree of significance	Contribution (%)
Model	0.19	9	0.021	7.40	0.0022	Significant	
V_c	0.044	1	0.044	15.56	0.0028		25.54
f	0.021	1	0.021	7.56	0.0205		12.40
d	0.092	1	0.092	32.93	0.0002		54.05
$V_c \times f$	0.000	1	0.000	0.000	1.000		0.00
$V_c \times d$	8.000E-4	1	8.000E-4	0.29	0.6046		0.50
$f \times d$	1.250E-3	1	1.250E-3	0.45	0.5191		0.70
V_c^2	6.875E-3	1	6.875E-3	2.46	0.1481		4.03
f^2	2.750E-4	1	2.750E-4	0.098	0.7604		0.16
d^2	4.400E-3	1	4.400E-3	1.57	0.2384		2.60
Residual Error	0.028	10	2.799E-3				0.02
Total	0.21	19					100

Table 8 ANOVA for tool wear in radial direction for MQL machining with textured tool

Source	Sum of squares	DF	Mean square	F-value	Prob>F	Degree of significance	Contribution (%)
Model	0.10	9	0.012	6.08	0.0047	Significant	
V_c	0.018	1	0.018	9.23	0.0125		19.22
f	0.014	1	0.014	7.55	0.0205		15.72
d	0.053	1	0.053	27.88	0.0004		58.05
$V_c \times f$	5.000E-5	1	5.000E-5	0.026	0.8747		0.05
$V_c \times d$	1.800E-3	1	1.800E-3	0.94	0.3547		1.95
$f \times d$	2.000E-4	1	2.000E-4	0.10	0.7530		0.21
V_c^2	2.114E-3	1	2.114E-3	1.11	0.3177		2.31
f^2	8.642E-4	1	8.642E-4	0.45	0.5166		0.94
d^2	1.420E-3	1	1.420E-3	0.74	0.4089		1.54
Residual Error	0.019	10	1.911E-3				0.01
Total	0.12	19					100

5.2. The effect of lubrication type on tool wear

Fig. 6 shows the microscopic images of the tool rake face for the same machining conditions but different lubrication modes for the micro-textured tool with a distance of 100μm. As expected, by injecting high-speed cutting fluid in the MQL method, the wear results recorded under the MQL method are less than the dry method. In the MQL, the cutting fluid particles are easily transferred to the tool-chip interface through micro-grooves that act as a micro-channel. By transferring fluid particles to an area where the stress is very high, lubrication between these two solid surfaces occurs in a hydrodynamic lubrication mode, as shown in Fig. 7. The friction coefficient shifts to smaller values [24]. By reducing the friction coefficient, reducing the generated heat in this area is not unexpected for the MQL mode. Knowing that generation of high levels of heat is one of the governing factors on the wear rate at the tool-chip contact surface, MQL methods may tend to reduce the generated heat (Fig. 6).

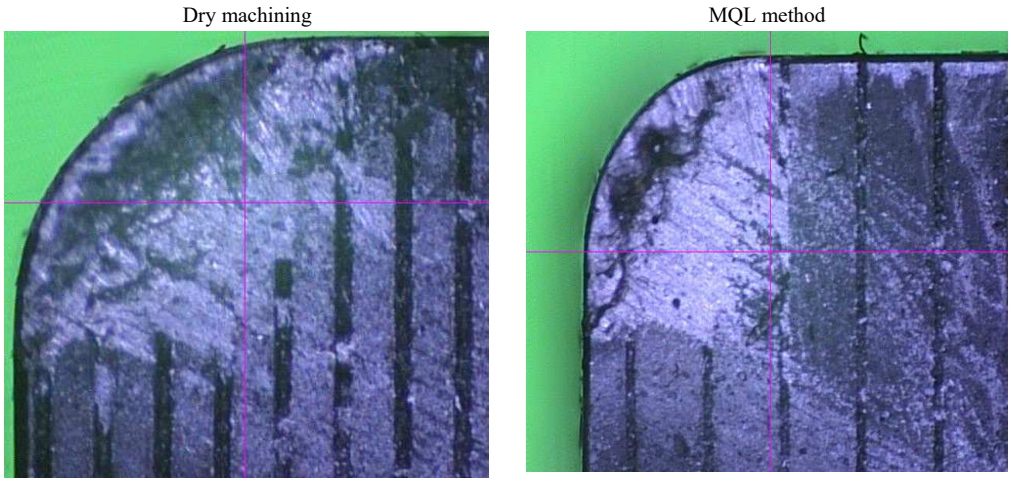

Fig. 6 Microscopic image of the tool rake face for both dry machining and minimum quantity lubrication method

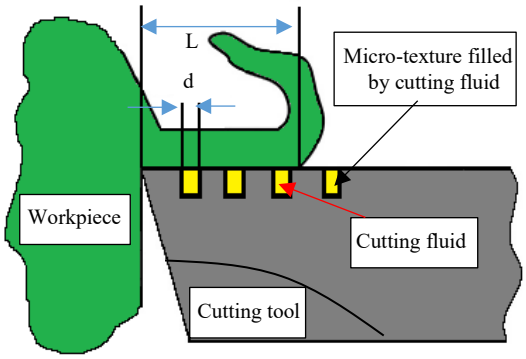

Fig. 7 Schematic image of lubrication technique on the textured tool

In summary, creating a micro-texture with a proper orientation towards the cutting edge on the tool rake face led to improvement in the chip removal performance due to the following three phenomena:

- The tool-chip contact surface (metal to the metal surface) was reduced, and less friction and heat were observed.
- More cutting fluid could be stored in the grooves, and consequently, better lubrication and cooling performance were observed during the machining process.
- The cutting fluid trapped inside the grooves could generate hydrodynamic pressure. This phenomenon led to the creation of the opposite force and separating the chips from the tool surface.

5.3. The effect of cutting speed on tool wear and surface roughness

Fig. 8 shows the effect of cutting speed on tool wear in different directions for MQL machining with the micro-textured tool. As can be seen in Fig. 8, tool wear decreases at a higher cutting speed. One of the reasons can be a slight increase in heat at a higher cutting speed. Consequently, a lower tendency of the chips to adhere to the tool surface may occur, which is the thermal softening mode. By reducing BUE

formation, the tool life increase and tool wear decrease. Therefore, it should be elevated heat generation at higher levels of cutting speed, which may negatively affect the tool performance, wear, and quality when machining aluminum. The effect of cutting speed on the tool wear in different directions for conventional tools is the same as for textured tools. Full details were presented in the appendix.

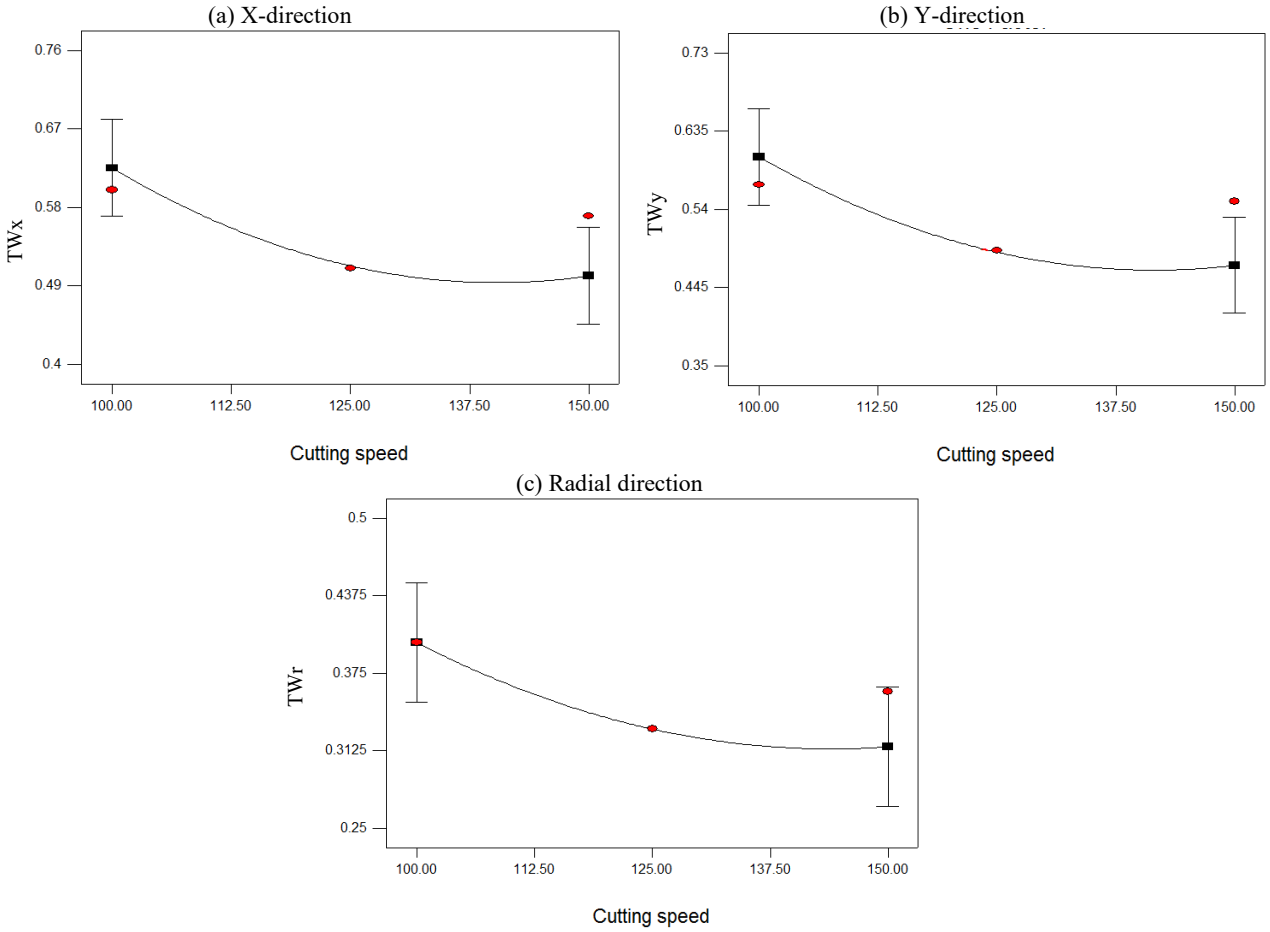

Fig. 8 The effect of cutting speed on tool wear in different directions during MQL machining with textured tool

As noted earlier, the average surface roughness (Ra) was used as the surface quality attribute. Fig. 9 shows the effect of cutting speed on Ra criterion under different machining modes. As the cutting speed increases, the number of engagements of the cutting edge with the material of the workpiece being removed increases, and less material is removed from the workpiece surface. This phenomenon led to improved surface quality by increasing the cutting speed, similar to the surface roughness under the Rz criterion. Comparing Fig. 9 with Fig. 8, it can be concluded that the effect of cutting speed is the same for both parameters. This phenomenon entirely proves that by reducing tool wear, surface roughness also decreases. In addition, the roughness value in the textured tool is less than the conventional tool. Therefore, by increasing the cutting speed, the volume of the workpiece material penetrated the grooves decreased, which may lead to tool wear

reduction in the three specified directions and surface roughness for both dry and MQL machining methods. Therefore, this indicates better efficiency of micro-texture at high cutting speeds.

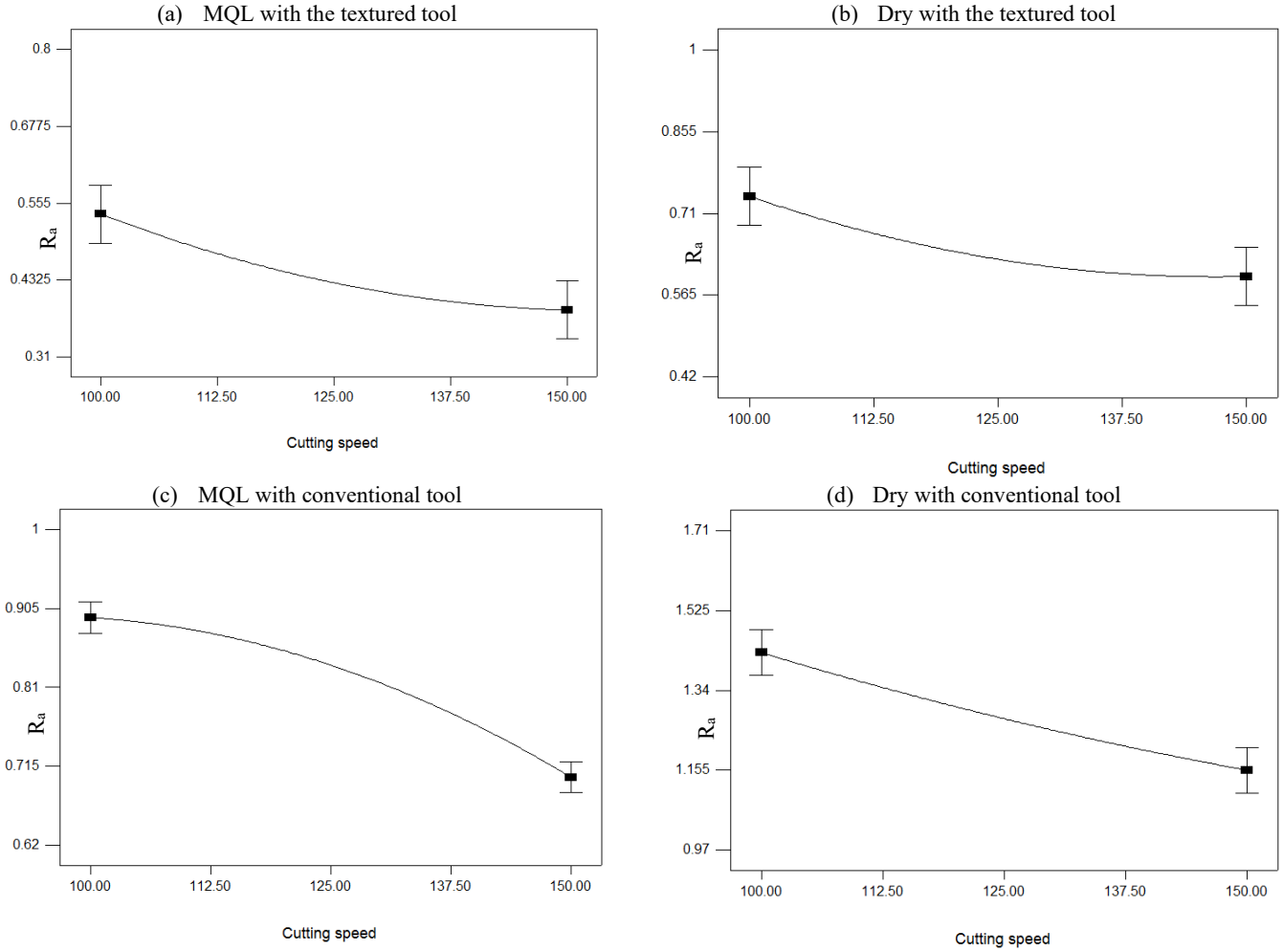

Fig. 9 the effect of cutting speed on surface roughness

Fig. 10 represents the microscopic image of the tool rake face to show the effect of cutting speed on wear for textured tools. According to Fig. 10, it can be concluded that by increasing cutting speed, the area under the wear curve also decreases on the tool rake face, which proves the abovementioned discussion. This phenomenon was observed for both dry and MQL modes and both textured and conventional tools.

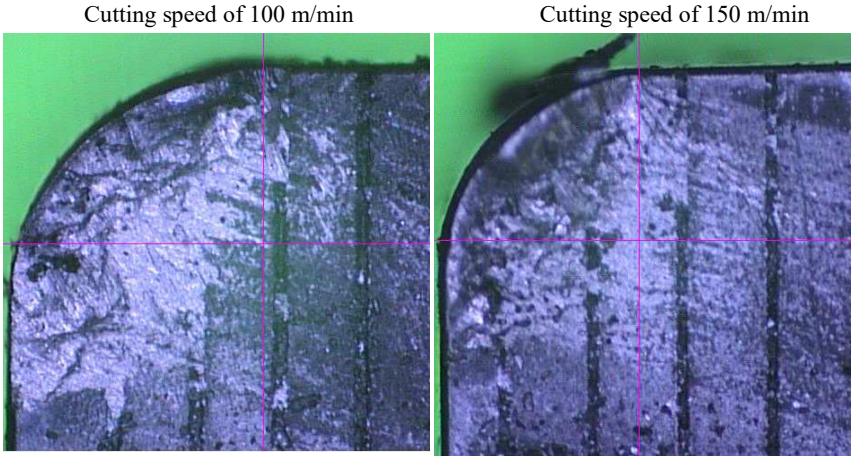

Fig. 10 Microscopic images of tool rake face at different cutting speed

5.4. The effect of feed rate on tool wear

As shown in Fig. 11, fed rate and cutting speed have opposite effects on the tool wear. In other words, at a higher feed rate, tool wear increases. As the feed rate increases, less time is given to the cutting edge to engage the workpiece surface. This increases the cutting force during the chip removal and makes the machining conditions more difficult, which results in an increase in the wear surface on the tool rake face. Fig. 11 shows the effect of feed rate on wear in different directions in MQL machining of micro-textured tools.

To investigate the simultaneous effects of input parameters machinability attributes, a surface contour diagram can be used. Fig. 12 shows the surface contour of the simultaneous effect of feed rate and cutting speed on tool wear in the Y and radial directions under MQL machining with textured tools. In the contour provided for wear in the y-direction, the best wear range was observed for cutting speeds around 137-150 m/min for a feed rate of 0.1 mm/rev. By increasing the feed rate up to 0.2 mm/rev, more wear is expected. At a higher level of feed rate (0.2 mm/rev) and lower level of cutting speed (100 m/min), the highest radial wear was observed (Fig. 12(b)).

(a) X-direction

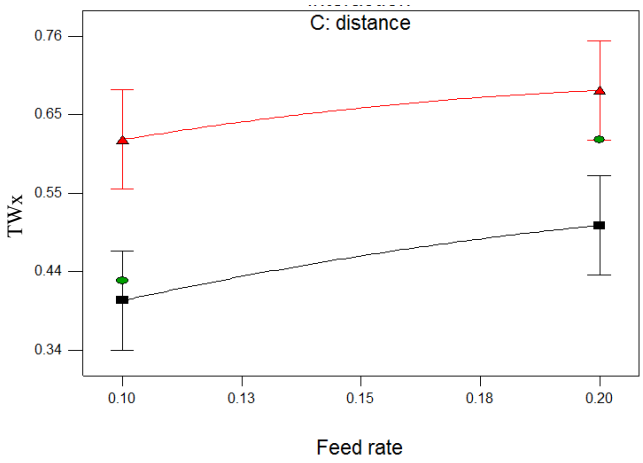

(b) Y-direction

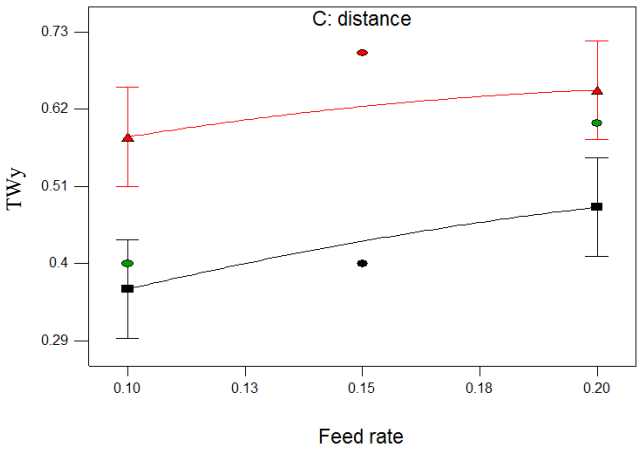

(c) Radial direction

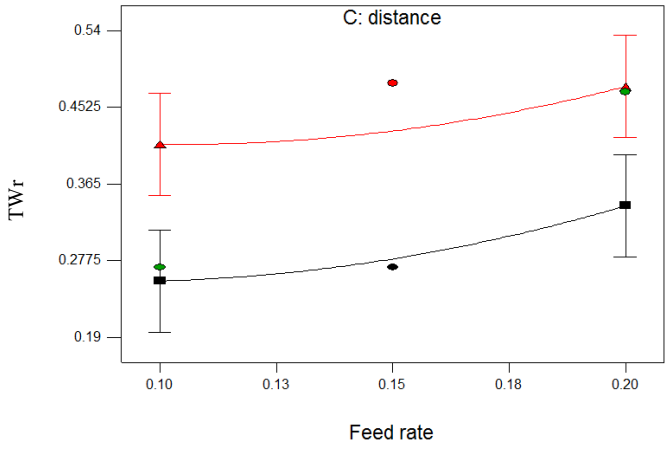

Fig. 11 The effect of feed rate on tool wear in different direction during MQL machining with textured tool

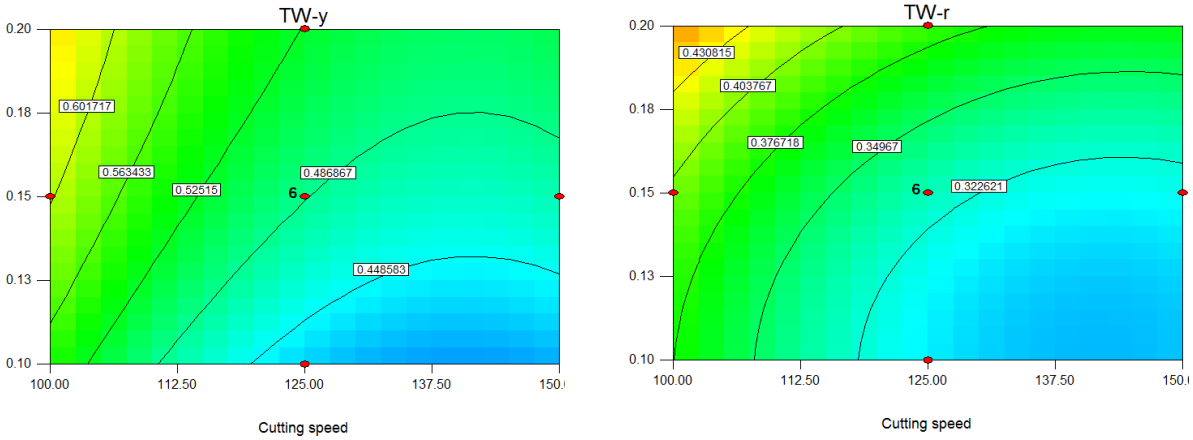

Fig. 12 Surface contour diagram of the simultaneous effect of feed rate and cutting speed on tool wear for MQL machining with textured tool

To prove the accuracy of surface contour images, microscopic images of the tool rake face were used. Fig. 13 shows the prepared microscopic images for different feed rates. As can be seen from Fig. 13, an increase in the surface area under adhesion wear can be seen by increasing the feed rate.

(a) Feed rate: 0.1 mm/rev (b) Feed rate: 0.2 mm/rev

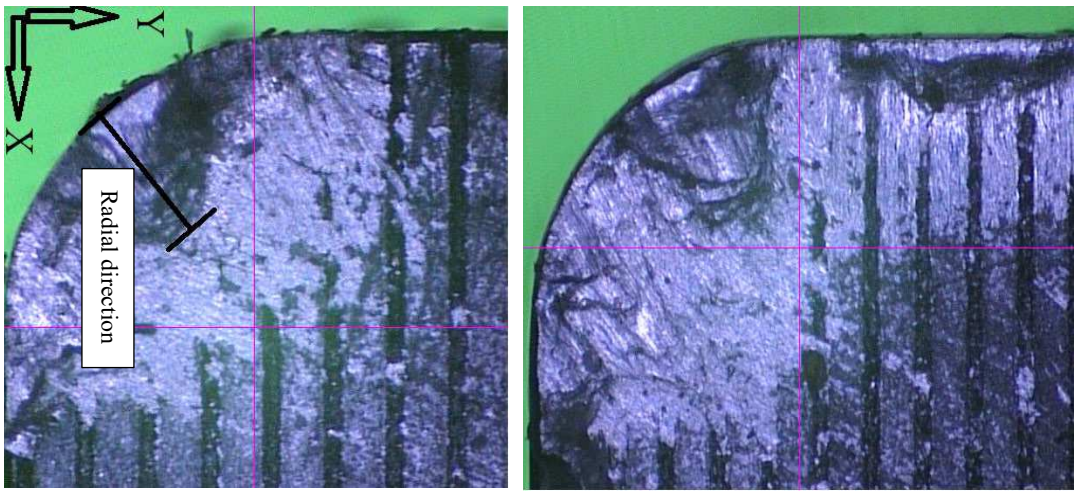

Fig. 13 Microscopic image of tool rake face at a different feed rate

5.5. The effect of grooves distance on tool wear

Fig. 14 shows three-dimensional surface graphs for interaction effects of grooves distance and the cutting speed on the tool wear in the X-direction under both dry and MQL machining. In both diagrams, it can be seen that the wear increases at the higher distance between the grooves. As the distance between the grooves increases, the density of these grooves or, in other words, the number of grooves in the unit surface decreases. Reducing the density of the grooves in the surface on which the chip reclines on the tool rake face reduces the impact of the micro-texture during machining. As the number of grooves decreases, less cutting fluid can be injected into the machining area. By reducing the volume of cutting fluid to the machining area, the quality of material removal deteriorates [25], and more tool wear in all directions can be observed. This phenomenon was observed under both MQL and dry machining. In other words, the presence of wear patterns with increasing grooves distance is the same for the two lubrication methods, and only the amount of wear in these two areas is different. These values have been improved for the MQL method. Fig. 14 indicates that the most negligible tool wear is achieved at the highest cutting speeds and the lowest grooves distance, i.e., at cutting speed of 150 m/min and distance of 100μm. By decreasing the cutting speed and increasing the distance of the groove, higher tool wear was achieved. This observation confirms the analysis of variance in which groove distance and cutting speed are the most influential parameters.

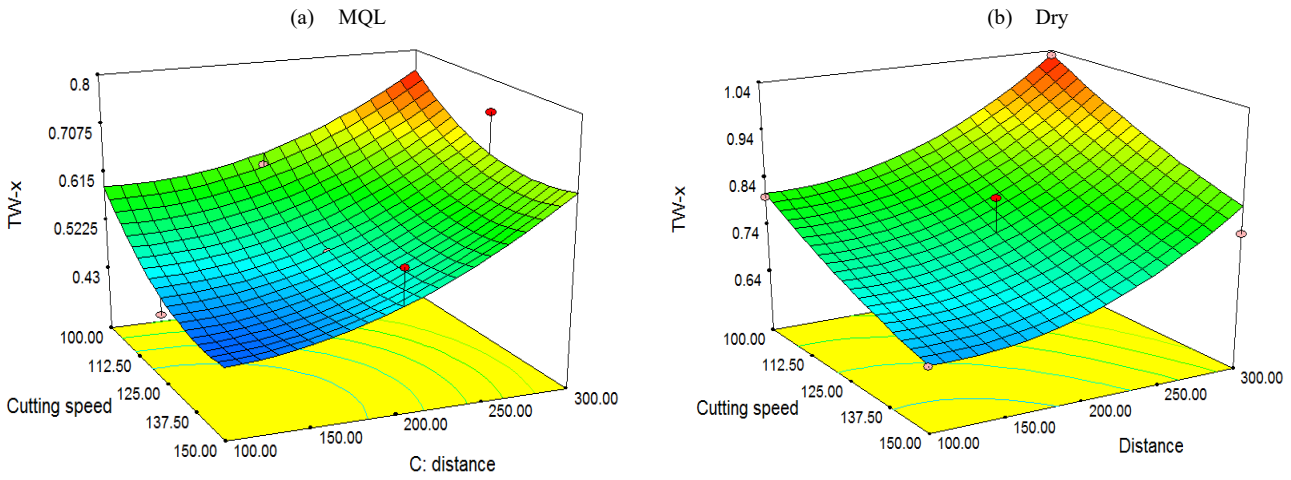

Fig. 14 3D graphs of interaction effects of grooves distance and the cutting speed on tool wear in X direction using different methods

6. Conclusion

In the present study, the effects of micro-textures and cutting parameters on the tool wear were studied in machining Al 7075. The following conclusions can be drawn from the study:

- The tool wear and surface roughness results for MQL machining were better than those recorded under dry mode. This phenomenon can be attributed to the better transfer of cutting fluid particles to the machining area in the MQL method.
- The recorded results under the micro-textured tool were better than those recorded under the non-textured tool in dry and MQL methods.
- Among the cutting parameters studied in this work, grooves distance had the highest effects on tool wear and surface roughness.
- By decreasing the grooves distance, tool wear and surface roughness were improved under dry and MQL methods.
- By increasing the cutting speed, the volume of the workpiece material penetrated the grooves decreased, which led to a reduction in tool wear and surface roughness for both machining methods. Therefore, this indicates better efficiency of micro-texture at high cutting speeds.
- The feed rate and cutting speed have opposite effects on tool wear and Ra. In other words, simultaneous optimization of the machinability attributes tends to be complex as input parameters have different effects on the responses.

Declarations

a. **Funding:** Not applicable
b. **Conflicts of Interest:** The authors declare no conflict of interest. The funders had no role in the design of the study, in the collection, analyses, or interpretation of data, in the writing of the manuscript, or in the decision to publish the results.
c. **Availability of data and material:** The authors confirm that the data supporting the findings of this study are available within the article [and/or] its supplementary materials.
d. **Code availability:** Not applicable
e. **Ethics approval:** Not applicable
f. **Consent to participate:** Not applicable
g. **Consent for publication:** All authors permit the publisher to publish the work.
h. **Author Contributions:** The research results in this work were presented in the M.S thesis of Mr. Sepehrikia. Mr. Musavi, the current Ph.D. student, helped him in experimental works and data analysis. Dr. Niknam and Dr.Davoodi also acted as the supervisors of Mr. Sepehrikia. All authors have read and agreed to the published version of the manuscript.

Reference

[1] Musavi S. H., Davoodi B., Nankali M., 2021, Assessment of Tool Wear and Surface Integrity in Ductile Cutting Using a Developed Tool, Arabian journal for science and engineering, https://doi.org/10.1007/s13369-021-05560-4.

[2] Rodrigues, S.P.; Alves, C.F.; Cavaleiro, A.; Carvalho, S.: Water and oil wettability of anodized 6016 aluminum alloy surface. Appl. Surf. Sci. 422, 430–442 (2017)

[3] Barari N, Niknam S A, Mehmanparast H (2019) Tool wear morphology and life under various lubrication modes in turning stainless steel 316L [J]. Transactions of the Canadian Society for Mechanical Engineering, 51: 1-10. DOI:10.1139/tcsme-2019-0051.

[4] /., Orra, K., Choudhury, S. K., 2018, Tribological aspects of various geometrically shaped micro-textures on cutting insert to improve tool life in hard turning process, Journal of Manufacturing Processes, 31, 502–513.

[5] Musavi SH, Davoodi B., 2021, Risk assessment for hazardous lubricants in machining industry. Environmental Science and Pollution Research, 28, 625–634. https://doi.org/10.1007/s11356-020-10472-1

[6] Martinez, I., Tanaka, R., Yamane, Y., Sekiya, K., Yamada, K., Ishihara, T., Furuya, S., 2016, Wear mechanism of coated tools in the turning of ductile cast iron having awide range of tensile strength, Precision Engineering, 47, 46-53.

[7] Musavi, S. H., Davoodi, B., Niknam, S. A., 2021, Eco-green machining of superalloy A286: Assessment of tool wear morphology and surface topology, Proceedings of the Institution of Mechanical Engineers, Part B: Journal of Engineering Manufacture, 235, 1–13.

[8] Kannan, S.; Ghosh, A.: Anti-friction and wetting behavior of a new polymer composite coating towards aluminum and dry machining of AA2024 alloy by coated end mills. J. Mater. Process. Technol. 252, 280–293 (2018).

[9] Davoodi B., Musavi S. H., Nankali M., 2017, Development a new cutting tool by changing the surface texture for increasing the machining performance. Modares Mechanical Engineering. 17(7), 441–450.
[10] Musavi S. H., Davoodi B., Nankali M., 2018, Creating the micro-grooves on tool rake face for improving the anti-wear properties**.** Modares Mechanical Engineering, 18, 1-10.
[11] Gomez-Parra, A., Alvarez-Alco, M., Salguero, J., Batista, M., Marcos, M., 2013, Analysis of the evolution of the Built-Up Edge and Built-Up Layer formationmechanisms in the dry turning of aeronautical aluminum alloys, Wear*,* 302, 1209–1218.
[12] Arulkirubakaran, D., Senthilkumar, V., Kumawat, V., 2016, Effect of micro-textured tools on machining of Ti–6Al–4V alloy: An experimental and numerical approach, Int. Journal of Refractory Metals and Hard Materials, 54, 165–177.
[13] Niketh, S., Samuel, G. L., 2017, Surface texturing for tribology enhancement and its application on drill tool for the sustainable machining of titanium alloy, Journal of Cleaner Production,167, 253-270.
[14] Obikawa, T., Kamio, A., Takaoka, H., Osad, A., 2011, Micro-texture at the coated tool face for high-performance cutting, International Journal of Machine Tools & Manufacture, 51, 966–972.
[15] Musavi S. H., Davoodi B., Eskandari B., 2019, Pre-cooling intensity effects on cooling efficiency in Cryogenic Turning, Arabian journal for science and engineering, 44: 10389-10396. DOI: 10.1007/s13369-019-04056-6.
[16] Feng, Y., Zhang, J., et al., 2017, Fabrication techniques and cutting performance of micro-textured self-lubricating ceramic cutting tools by in-situ forming of Al2O3-TiC, International Journal of Refractory Metals & Hard Materials, 68, 121-129.
[17] Zhang, K., Deng, J., Sun, J., Jiang, Ch., Liu, Y., Chen, Sh., 2015, Effect of micro/nano-scale textures on anti-adhesive wear propertiesof WC/Co-based TiAlN coated tools in AISI 316 austenitic stainless steel cutting, *Applied Surface Science,* 355, 602–614.
[18] Kummel, J., Braun, D., Gibmeier, J., Schneider, J., Greiner, Ch., Schulze, V., Wanner, A., 2015, study on micro-texturing of uncoated cemented carbide cutting tools for wear improvement and built-up edge stabilization, 215, 62-70.
[19] Fang, Z., Obikawa, T., 2017, Cooling performance of micro-texture at the tool flank face under high-pressure jet coolant assistance, *Precision Engineering,* 49, 41-51.
[20] Musavi SH, Davoodi B, Eskandari B. Evaluation of surface roughness and optimization of cutting parameters in turning of AA2024 alloy under different cooling-lubrication conditions using RSM method. Journal of Central South University, 2020, 27(6): 1714-1728.
[21] U. Natarajan, P. Periyanan, S. Yang, Multiple-response optimization for micro-endmilling process using response surface methodology, Int. J. Adv. Manuf. Technol. 56 (2011) 177–185.
[22] Davoodi, B., Eskandari, B., 2015, Tool wear mechanisms and multi-response optimization of tool life and volume of material removed in turning of N-155 iron-nickel-base superalloy using RSM, Measurement, 68, 286-294.
[23] D.C. Montgomery, D.C. Montgomery, D.C. Montgomery, Design and Analysis of Experiments, Wiley, New York, 1984.

[24] Davoodi B., Musavi S. H., 2016, An experimental investigation of the effect of lubrication method on surface roughness and cutting fluid consumption in machining of super alloys, Modares Mechanical Engineering, 16, 343-352.
[25] Musavi S. H., Davoodi B., Niknam S. A. 2019, Effects of reinforced nanofluid with nanoparticles on the cutting tool wear morphology, Journal of Central South University, 26(5), 1050–1064.

Appendix

Tables 9 and 10 show the values of measured tool wear in different directions using dry and MQL machining modes.

Table 9 Matrix L20 of response surface methodology of wear results in the dry method using the textured tool

Test number	Matrix L20			Blocks	F_1 V_c (m/min)	F_2 f (mm/rev)	F_3 d (μm)	Tool wear		
	F_1	F_2	F_3					TW-x(mm)	TW-y (mm)	TW-r (mm)
1	0.000	0.000	1.633	2	125	0.15	300	0.65	0.85	0.92
2	0.000	0.000	0.000	1	125	0.15	200	0.70	0.68	0.47
3	0.000	0.000	0.000	2	125	0.15	200	0.68	0.65	0.45
4	0.000	0.000	-1.633	2	125	0.15	100	0.61	0.58	0.42
5	-1.633	0.000	0.000	2	100	0.15	200	0.75	0.71	0.45
6	1.000	1.000	-1.000	1	150	0.2	100	0.64	0.60	0.42
7	-1.000	1.000	-1.000	1	100	0.2	100	0.80	0.73	0.49
8	1.000	-1.000	-1.000	1	150	0.1	100	0.57	0.55	0.40
9	0.000	0.000	0.000	1	125	0.15	200	0.70	0.66	0.48
10	1.633	0.000	0.000	2	150	0.15	200	0.69	0.65	0.52
11	0.000	1.633	0.000	2	125	0.2	200	0.83	0.73	0.60
12	0.000	0.000	0.000	1	125	0.15	200	0.70	0.65	0.47
13	1.000	-1.000	1.000	1	150	0.1	300	0.78	0.75	0.55
14	0.000	0.000	0.000	2	125	0.15	200	0.69	0.65	0.46
15	1.000	1.000	1.000	1	150	0.2	300	0.79	0.75	0.58
16	-1.000	-1.000	1.000	1	100	0.1	300	0.92	0.85	0.56
17	0.000	-1.633	0.000	2	125	0.1	200	0.60	0.59	0.42
18	0.000	0.000	0.000	1	125	0.15	200	0.71	0.67	0.46
19	-1.000	1.000	1.000	1	100	0.2	300	1.03	0.95	0.70
20	-1.000	-1.000	-1.000	1	100	0.1	100	0.75	0.70	0.47

Table 10 Matrix of response surface methodology of wear results using conventional tool

Test number	F_1 V_c (m/min)	F_2 f (mm/rev)	MQL			Dry		
			TW-x(mm)	TW-y (mm)	TW-r (mm)	TW-x(mm)	TW-y (mm)	TW-r (mm)
1	150	0.1	0.65	0.6	0.5	0.85	0.81	0.74
2	100	0.15	1.06	0.94	0.79	1.32	1.22	1.15
3	100	0.1	0.95	0.9	0.71	1.25	1.20	1.09
4	125	0.15	0.84	0.78	0.75	1.07	1.05	0.82
5	150	0.15	0.72	0.67	0.57	0.92	0.90	0.87
6	125	0.15	0.81	0.74	0.74	1.06	1.02	0.89
7	125	0.15	0.85	0.75	0.73	1.10	1.07	0.91
8	150	0.2	0.80	0.74	0.67	1.04	1.00	1.00
9	125	0.15	0.85	0.79	0.75	1.10	1.09	0.90
10	125	0.2	0.92	0.82	0.78	1.15	1.10	0.93
11	125	0.15	0.83	0.76	0.75	1.08	1.05	1.05
12	100	0.2	1.1	1	0.85	1.40	1.25	1.17
13	125	0.1	0.8	0.76	0.70	1.03	0.97	0.80

The final tool wear models in different directions for dry machining with the textured tool, MQL machining with the conventional tool, and dry machining with the conventional tool are presented in Equations (7) to (9), Equations (10) to (12), and Equations (13) to (15), respectively:

$$TWx = 1.257 - 0.008V_c + 0.68545f - 0.0011d - 0.008V_cf - 0.000002V_cd + 0.000fd + 0.0000247{V_c}^2 + 4.18182f^2 + 0.00000605d^2 \quad (7)$$

$$TWy = 1.246 - 0.0092V_c + 1.54f - 0.00116d - 0.008V_cf - 0.000001V_cd + 0.0005fd + 0.000032{V_c}^2 + 0.000f^2 + 0.0000055d^2 \quad (8)$$

$$TWr = 0.292 + 0.0042V_c - 0.458f - 0.0014d - 0.011V_cf + 0.0000005V_cd + 0.00325fd - 0.0000138{V_c}^2 + 6.5454f^2 + 0.0000041d^2 \quad (9)$$

$$TWx = -0.26362 + 0.013701V_c + 4.75557f - 0.0134V_cf + 0.00006209{V_c}^2 - 4.72414f^2 \quad (10)$$

$$TWy = -3.84953 + 0.13122V_c + 31.78626f - 0.0622V_cf - 0.0005935{V_c}^2 - 39.7931f^2 \quad (11)$$

$$TWr = 2.34057 - 0.02034V_c + 0.77931f + 0.000V_cf + 0.000056{V_c}^2 + 2.06897f^2 \quad (12)$$

$$TWx = 3.1046 - 0.025485V_c - 0.83218f + 0.008V_cf + 0.0000662{V_c}^2 + 4.55172f^2 \quad (13)$$

$$TWy = 2.53017 - 0.017221V_c - 1.25287f + 0.028V_cf + 0.00002648{V_c}^2 - 3.37931f^2 \quad (14)$$

$$TWr = 5.44098 - 0.06825V_c - 1.0885f + 0.036V_cf + 0.00023{V_c}^2 - 6.48276f^2 \quad (15)$$

Tables 11 and 12 show the values of measured surface roughness in different machining modes.

Table 11 Matrix L20 of response surface methodology of roughness results in dry method using textured tool

Test number	Matrix L20			Blocks	F_1 V_c (m/min)	F_2 f (mm/rev)	F_3 d (μm)	Roughness	
	F_1	F_2	F_3					R_a (μm)	Rz (μm)
1	0.000	0.000	1.633	2	125	0.15	300	0.869	6.198
2	0.000	0.000	0.000	1	125	0.15	200	0.614	3.611
3	0.000	0.000	0.000	2	125	0.15	200	0.608	3.598
4	0.000	0.000	-1.633	2	125	0.15	100	0.564	3.309
5	-1.633	0.000	0.000	2	100	0.15	200	0.698	4.789
6	1.000	1.000	-1.000	1	150	0.20	100	0.597	3.703
7	-1.000	1.000	-1.000	1	100	0.20	100	0.772	5.866
8	1.000	-1.000	-1.000	1	150	0.10	100	0.421	2.631
9	0.000	0.000	0.000	1	125	0.15	200	0.623	3.607
10	1.633	0.000	0.000	2	150	0.15	200	0.692	3.994
11	0.000	1.633	0.000	2	125	0.20	200	0.716	5.127
12	0.000	0.000	0.000	1	125	0.15	200	0.617	3.601
13	1.000	-1.000	1.000	1	150	0.10	300	0.611	3.982
14	0.000	0.000	0.000	2	125	0.15	200	0.621	3.608
15	1.000	1.000	1.000	1	150	0.20	300	0.739	5.448
16	-1.000	-1.000	1.000	1	100	0.10	300	0.769	5.352
17	0.000	-1.633	0.000	2	125	0.10	200	0.497	2.874
18	0.000	0.000	0.000	1	125	0.15	200	0.613	3.584
19	-1.000	1.000	1.000	1	100	0.20	300	0.998	6.632
20	-1.000	-1.000	-1.000	1	100	0.10	100	0.539	3.274

Table 12 Matrix of response surface methodology of roughness results using conventional tool

Test number	F_1 V_c (m/min)	F_2 f (mm/rev)	MQL		Dry	
			R_a (μm)	Rz (μm)	R_a (μm)	Rz (μm)
1	150	0.1	0.621	4.317	0.977	6.807
2	100	0.15	0.869	6.187	1.431	8.992
3	100	0.1	0.787	5.519	1.243	7.312
4	125	0.15	0.841	6.009	1.265	7.641
5	150	0.15	0.693	4.927	1.185	7.757
6	125	0.15	0.849	6.002	1.168	7.635
7	125	0.15	0.841	6.011	1.272	7.649
8	150	0.2	0.762	5.412	1.402	8.849
9	125	0.15	0.834	6.008	1.270	7.640
10	125	0.2	0.883	6.389	1.591	9.202
11	125	0.15	0.837	6.010	1.274	7.645
12	100	0.2	0.995	6.925	1.704	9.768
13	125	0.1	0.733	5.268	1.127	7.102

The final roughness models for MQL machining with textured tool, dry machining with textured tool, MQL machining with conventional tool and dry machining with conventional tool are presented in Equations (16) to (19), respectively:

$$R_a = 1.047 - 0.0129V_c + 3.909f - 0.00096d - 0.013V_cf - 0.0000066V_cd - 0.0014fd + 0.000053{V_c}^2 - 3.1818f^2 + 0.0000078d^2 \quad (16)$$

$$R_a = 0.8221 - 0.015V_c + 9.9377f - 0.0004d - 0.0158V_cf - 0.000006V_cd - 0.0013fd + 0.000065{V_c}^2 - 19.10909f^2 + 0.00000622d^2 \quad (17)$$

$$R_a = -0.26362 + 0.013701V_c + 4.75557f - 0.0134V_cf + 0.00006209{V_c}^2 - 4.72414f^2 \quad (18)$$

$$R_a = 2.16109 - 0.0110781V_c - 2.73931f - 0.0072V_cf + 0.00002692{V_c}^2 + 27.13103f^2 \quad (19)$$